

Sonoluminescence from Ultra-High-Temperature and High-Pressure Cavitation and its Effect on Surface Modification of Cr-Mo Steel

Toshihiko Yoshimura^{1*}, Daisaku Maeda¹, Takayuki Ogi¹, Fumihiro Kato¹ and Masataka Ijiri²

¹Department of Mechanical Engineering, Sanyo-Onoda City University, 1-1-1 Daigaku-dori, Sanyo-Onoda, Yamaguchi, 756-0884, Japan

²Department of Advanced Machinery Engineering, Tokyo Denki University, 5 Senju-Asahi-Cho, Adachi-Ku, Tokyo, 120-8551, Japan

Abstract

Sonoluminescence from various types of cavitation bubbles, namely those of Water Jet Cavitation (WJC), Water Jet Cavitation with a Swirl Flow Nozzle (SFN-WJC), Multifunction Cavitation (MFC), Ultrasonic Cavitation (UC), and Ultrahigh-Temperature and High-Pressure Cavitation (UTPC), was investigated. The sonoluminescence measurements were compared with the surface modification characteristics imparted to Cr-Mo steel. The luminescence intensity of the various types of cavitation was measured using two types of photon counting head, whose detection sensitivity depends on the wavelength range. UTPC had the highest light intensity, followed by MFC, UC, SFN-WJC, and WJC. The temperature inside the bubbles from the various types of cavitation could be estimated using the black-body emission method based on Planck's law and the emission intensity, which was corrected for the sensitivity of the detector. UTPC, which had high luminosity and could treat surfaces at high temperatures, was found to increase compressive residual stress and decrease surface roughness compared to WJC and SFN-WJC, which had low luminosity and are forms of cold working. At higher cavitation temperature, more corrosion-resistant and oxidation-resistant films form on a steel surface. The magnitude of luminescence intensity for a cavitation process corresponds to the magnitude of corrosion potential (surface potential), which indicates corrosion resistance.

Keywords: Multifunction cavitation • Water jet cavitation • Ultrasonic cavitation • High- pressure high-temperature cavitation • Sonoluminescence • Surface modification

Introduction

Sonoluminescence refers to the light emission that occurs when bubbles in a liquid subjected to ultrasonic waves collapse. The light emission mechanism is still not fully understood. When a liquid is irradiated with ultrasonic waves, numerous bubbles are generated due to cavitation. The bubbles expand when the ultrasonic pressure becomes negative, and contract when it becomes positive. In particular, bubbles with a size close to the resonance diameter [1] of the ultrasonic waves shrink at close to the speed of sound, and are instantaneously heated to several thousand kelvins or more by the effect of adiabatic compression. At this time, light emission from atoms and molecules thermally excited by high temperature and chemiluminescence from radicals occur inside the bubble. In addition, plasma is emitted from ionized gas in the strongly compressed bubbles. Molecules generated in the high-temperature field in the bubbles dissolve into the liquid and cause various sonochemical reactions (especially in water, where OH reactions occur rapidly). The chemiluminescence that occurs at this time contributes to sonoluminescence, which is a pulse emission with a duration of tens to hundreds of picoseconds. The light emission is weak, requiring a dark room to be observed. However, if a luminescent (chemiluminescent) substance such as luminol is added to the liquid, relatively strong luminescence occurs. In Single-Bubble Sonoluminescence (SBSL) [2,3] light emission is precisely synchronized with the applied ultrasonic waves. Strong light emission also occurs in liquids with dissolved noble gases. Heavy noble gases, such as xenon and argon, emit more light. Ultrasonic waves are irradiated into the well-degassed liquid to create

a standing wave, in which a single bubble created by a syringe is trapped. The light emission that occurs at this time is SBSL.

SBSL bubbles are very hot because they are strongly compressed while maintaining their spherical shape. SBSL has a broad continuous spectrum similar to that of black-body radiation; no structures derived from atoms and molecules appear. When ultrasonic waves are applied to a liquid containing a large amount of gas, light is emitted from many bubbles. This is called Multi-Bubble Sonoluminescence (MBSL) [4-6]. When many bubbles vibrate at the same time, the bubble shape is distorted due to the interaction between bubbles, or the bubble vibration is disturbed. Because these effects often prevent the collapse of bubbles, MBSL emits light at a lower temperature than SBSL. Giri and Arakeri reported that the spectra of MBSL are similar to those of SBSL when the acoustic amplitude is large enough [7]. The MBSL spectra of water in the presence of xenon resemble SBSL spectra [8]. MBSL has a broad continuous spectrum similar to that of black-body radiation, with band spectra and line spectra derived from atoms and molecules.

Cavitation is a physical phenomenon in which bubbles are generated and disappear in a short time due to a pressure difference in a liquid flow. It was first observed as air bubbles that eroded components such as those in fluid machinery and ships, and was thus suppressed. More recently, various types of cavitation have been utilized in several fields.

In Water Jet Cavitation (WJC), also called flow cavitation, the pressure at the time of bubble collapse is high [9] and the mechanical action is strong. As an alternative to conventional surface treatments such as shot peening [10] and particle peening, [11] WJC can be used as a peening technique [12-14]. For example, WJC has been used for imparting compressive residual stress to the component materials of a nuclear power plant [15] and for surface hardening. Ultrasonic Cavitation (UC), also called vibration cavitation, [16] has strong thermal and electrochemical actions. It is applied in surface cleaning, chemical, biological, and medical fields. Microbubbles and nanobubbles, which have a strong chemical action, are applied to sterilization, water purification, medicine, and beauty treatments. Our group combined the features of WJC and UC to create Multifunction Cavitation (MFC), [17-19] which uses large bubbles at high temperature and pressure (International PCT published patent WO2016136656A1,

*Address for Correspondence: Toshihiko Yoshimura, Department of Mechanical Engineering, Sanyo-Onoda City University, 1-1-1 Daigaku-dori, Sanyo-Onoda, Yamaguchi, 756-0884, Japan, Tel: +81 836 88 4562, Fax: +81 8-884562, E-mail: yoshimura-t@rs.socu.ac.jp

Copyright: © 2020 Yoshimura T, et al. This is an open-access article distributed under the terms of the Creative Commons Attribution License, which permits unrestricted use, distribution, and reproduction in any medium, provided the original author and source are credited.

US registered patent, Inventor: Toshihiko Yoshimura, Assignee: SANYO-ONODA CITY PUBLIC UNIVERSITY, Patent No.: US 10,590,966 B2, Date of Patent: Mar.17, 2020) [20]. A bubble in MFC has a radius of 100 μm or more, a collapse pressure of 1000 MPa or more, and an interior temperature of several thousand kelvins [21]. In previous studies, a Swirl Flow Nozzle (SFN) was installed on a water jet nozzle that generates MFC, and ultrahigh-temperature and High-Pressure Cavitation (UTPC) [22,23] was developed to increase the size and number of bubbles. Using MFC and UTPC, we previously modified the surface of various metal materials, [24] nanoprocessed a photocatalyst powder, and improved photocatalytic properties [19,22]. However, it is unclear whether the bubble temperature of MFC or UTPC is sufficient to improve the functionality of various materials.

In this study, the light emitted during the collapse of a bubble in WJC, SFN-WJC, MFC, UC, and UTPC was measured with a photodetector to estimate the temperature inside the bubble. Furthermore, the relationship between the mechanical strength and corrosion resistance of low-alloy steel and bubble temperature was examined.

Material and Method

Experimental

A high-pressure pump was used in the experiment (MW7HP40L, MARUYAMA EXCELL Co., Ltd., power: 11 KW, pressure: 35 MPa, discharge rate: 15 L/min). The diameter of the water jet nozzle was Φ 0.8 mm and the actual flow rate was about 7 L/min. As shown in (Figure 1), when high-pressure water is injected from a nozzle into water, the water jet is irradiated with ultrasonic waves in the vertical direction. A large-output oscillator was used for this experiment. When ultrasonic waves are generated in water, the sound pressure of longitudinal waves changes. When ultrasonic waves are used for cleaning, bubble nuclei several microns in size that originally float in the water alternate between isothermal expansion and adiabatic compression, [19,25,26] with the temperature inside the bubbles reaching 2,000 K to 5,000 K. A high-temperature reaction field forms and removes contaminants, such as oils and fats, attached to the surface during bubble collapse. The bubble nucleus expands isothermally when the sound pressure created by the ultrasonic waves is low, contracts rapidly when the sound pressure is high, and emits light when the bubble collapses. This is called MBSL.

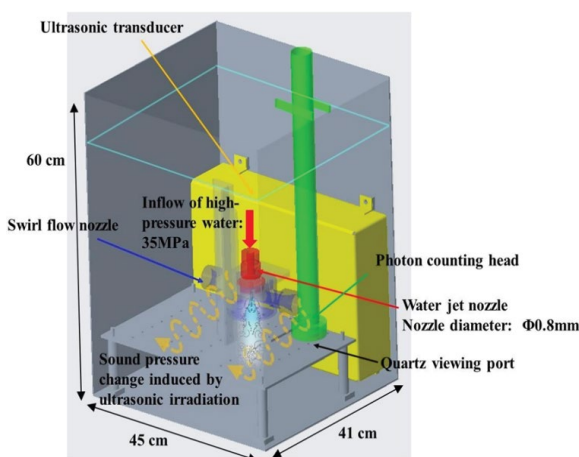


Figure 1. Schematic diagram of processing equipment for UTPC and method used for light intensity measurement.

An ultrasonic transducer was used in the experiment (WD-1200-28T, WS-1200-28N, HONDA ELECTRONICS CO., LTD., power: 1200 W, frequency: 28 kHz). The maximum output is 1200 W in single mode and 800 W in dual mode. Previous research [27] found that dual mode provides higher compressive residual stress and corrosion resistance, so in this research, dual mode was used (maximum output: 800 W).

In WJC, a large bubble with a radius of about 100 μm is generated when the static pressure becomes lower than the saturated vapor pressure due to an increase in the dynamic pressure at the center of the jet. In addition, a circulating vortex is generated around the jet. When the pressure at the center of the vortex becomes lower than the saturated vapor pressure, bubbles are generated. Then, when a WJC bubble approaches a material surface, it becomes a flat microjet that indents the surface. The shockwave hits the surface and plastically deforms it. The pressure is about 1,000 MPa. After the bubbles have disappeared, the surface has a compressive residual stress, which is applied by the elastic constraint from the surroundings. In addition, the surface is work-hardened and the mechanical strength is improved. This surface modification technique is called water jet peening. WJC bubbles irradiated with ultrasonic waves alternate between isothermal expansion and heat insulation compression, similar to the case for bubble nuclei, and large bubbles with hot spots [2,3,16,28] and high-temperature and-pressure microjets are generated.

An SFN [22,23] was attached to the water jet nozzle to increase the temperature and pressure of MFC (Figure 1). In the SFN, surrounding water flows in from the inflow hole due to a decrease in the static pressure at the outlet of the water jet nozzle, and a swirl flow forms. Because the pressure at the center of the swirl flow is further reduced, WJC bubbles expand and the number of bubbles increases because the cavitation number decreases. When many large bubbles from an SFN are irradiated with ultrasonic waves, the expansion and contraction rate of the bubbles increases, generating UTPC [22,23]. WJC is a form of cold working, whereas UTPC is a form of hot working because its microjet hits the surface. Therefore, it can be considered to be microforging. The pressure in an SFN with two holes is lower than that in an SFN with one hole. The compressive residual stress applied to the surface and the corrosion resistance thus increase when two holes are used. In this experiment, light emission from the various types of cavitation during surface modification was measured using two types of photon counting head.

The setup used to measure the emission intensity from multi-bubble cavitation is shown in Figure 1. A pipe with a quartz viewing port with high transmittance for vacuum usage was fixed at a position close to the ultrasonic vibrator and the SFN, and the emitted photons were measured.

Figure 2 shows the light emission measurement and cavitation processing conditions. At the time of light emission measurement, the processing equipment was covered with a dark curtain to prevent light from the surroundings from entering. Even in this dark state, several hundred photons were detected per second because of the high photomultiplier sensitivity. In the case of only ultrasonic waves (Figure 2a), a water jet does not form.

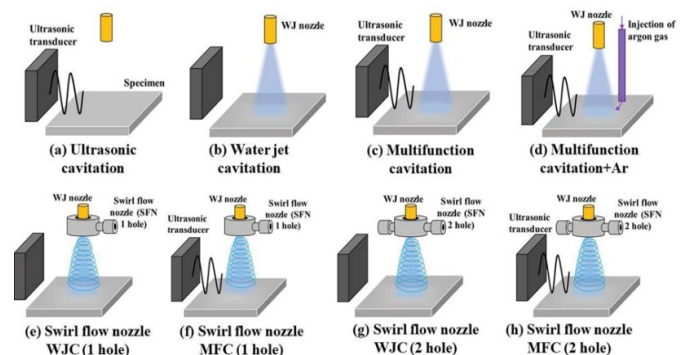


Figure 2. Various conditions of cavitation processing during photon counting and surface working.

Under all conditions, the stand-off distance (i.e., the water jet nozzle to specimen distance) was 65 mm. The discharge pressure of all water jet pumps was 35 MPa. In UC (Figure 2a), MFC (Figure 2c and 2d), and SFN-MFC (Figure 2f and 2h), dual model was used (ultrasonic output: 800 W). WJC bubbles contain water vapor, oxygen and hydrogen thermally

decomposed by the water vapor, nitrogen entering from the bubble wall, and other components. If alternating expansion and contraction is induced by ultrasonic waves, argon rectification, [29] the incorporation of the 1% argon contained in the atmosphere, will eventually occur. In this study, we investigated the change of luminescence intensity by injecting argon gas into the water tank (Figure 2d). The swirl velocity in the SFN with two inflow holes (Figure 2h) is larger than that in the SFN with one inflow hole (Figure 2f), and as a result, the bubble temperature with two inflow holes due to ultrasonic irradiation is considered to be higher. The effect of the number of inflow holes on light emission intensity was also investigated.

Figure 3 shows a schematic diagram of microjets under various processing conditions based on the results of our previous research [23]. A microjet is a cavitation bubble that approaches a material surface. The bubble deforms from a spherical shape to a flat shape in a short time (about 100 μ s) and strikes with a shockwave that pierces the surface. This phenomenon is believed to occur even when bubbles come close to each other. In UC, because the bubbles are as small as a few μ m, the shockwave applied to the surface is small, but a high temperature reaction field called a hot spot is formed by the isothermal expansion and adiabatic compression of the bubbles. Therefore, many photons are emitted from the bubbles and the emission intensity is high. In contrast, WJC and SFN-WJC have a large bubble radius (several hundred μ m) and a large shockwave. Because the bubbles do not emit ultrasonic waves, the temperature inside them is low and the emission intensity is low. The surface is plastically deformed by the shockwave, and after the disappearance of the bubbles, a compressive residual stress is applied by the elastic restraint from the surroundings. Many dislocations form on the surface. Voids and defects due to plastic deformation also form. Because MFC irradiates WJC bubbles with ultrasonic waves, the collapse pressure increases and hot spots form in large bubbles, resulting in higher temperature and emission intensity than those for UC. Although many dislocations are generated on the surface, recovery occurs because the surface temperature rises, and the dislocations disappear from the crystal grain boundaries and the surface due to the increased motion of the dislocations. It is considered that the impact pressure, bubble temperature, and emission intensity are further increased by adding an SFN, which increases the number of bubbles and bubble size. Because UTPC is a form of hot working, cracks do not occur directly under the surface, unlike for WJC, recovery and recrystallization occur, and dislocation generation and disappearance are balanced. Preexisting cracks also disappear.

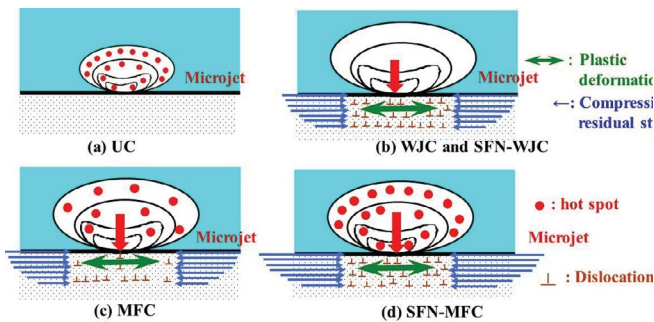


Figure 3. Microjet generated under various processing conditions.

Results and Discussion

Figure 4 shows the measurement results of light intensity for various types of cavitation obtained using photon counting head H9319-01. The gate time for measuring photons was set to 500 ms and measurements were conducted for about 2 minutes. The number of measured photons increases in the order of WJC, UC, MFC, and UTPC (SFN2-MFC). The photon counting head was equipped with a photomultiplier tube. When one photon emitted from a bubble enters the photomultiplier, an electron avalanche is induced and the electrons are detected as a single signal intensity. When argon gas is injected under MFC measurement conditions (Figure 2d), the emission intensity increases, though large fluctuations can

be seen. This is considered to be due to the fact that even in MFC, which includes multiple bubbles at high temperature and high pressure, the argon gas enters the bubbles, increasing emission intensity.

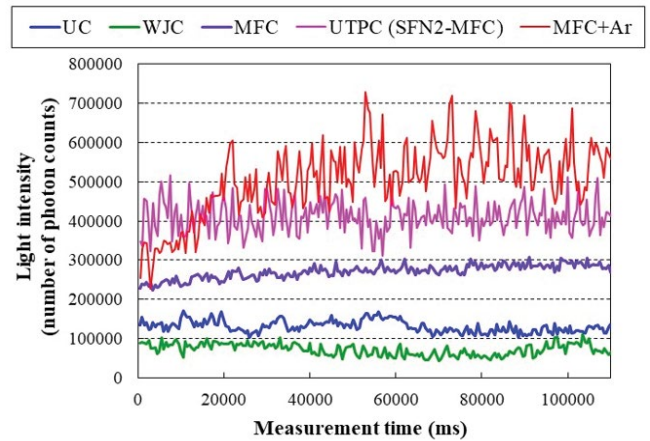


Figure 4. Measurement results of light intensity for various types of cavitation obtained using photon counting head H9319-01.

The relationship between the SFN and light intensity obtained using photon counting head H9319-01 is shown in Figure 5. SFN2-MFC (two inflow holes) has a higher emission intensity than that of SFN1-MFC (one inflow hole). This is due to the fact that with two holes, the flow velocity in the SFN is higher and the size of the WJC bubble, expansion/compression ratio, and bubble interior temperature are increased. Consequently, the number of emitted photons is increased.

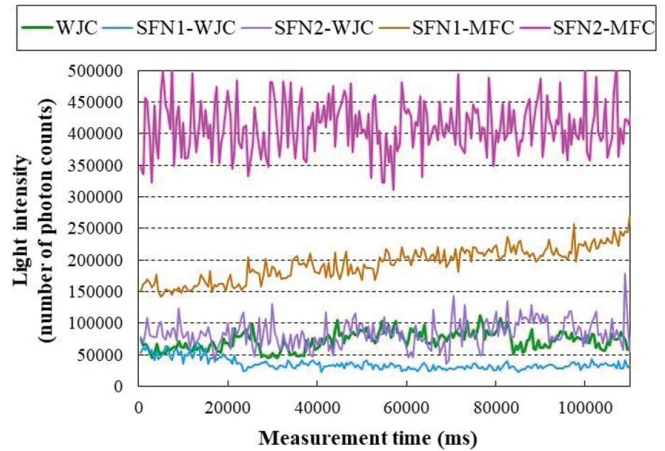


Figure 5. Relationship between SFN and light intensity obtained using photon counting head H9319-01.

Figure 6 shows the measurement results of light intensity for various types of cavitation obtained using photon counting head H9319-02. The gate time for measuring photons was set to 500 ms and measurements were conducted for about 2 minutes. The number of measured photons increases in the order of WJC, UC, UTPC (SFN2-MFC), and MFC. Unlike the results obtained using photon counting head H9319-01, the emission intensity of MFC is higher than that of UTPC (SFN2-MFC). As shown in Figure 1, for MFC and UTPC, cavitation can be measured only at the position where the bubble is ejected after the bubble collides with the specimen using the photon counting head. Because the photon counting head has a small light receiving area (a circle with a 25 mm diameter), the photons from the entire cavitation stream could not be measured. In addition, because the SFN has an inflow hole, the photon counting head cannot be set close to the surface that is actually modified, which limits the emission measurement from UTPC. Therefore, it is considered that the UTPC temperature is theoretically higher than that for MFC in the modified region of the surface. The photon counting head can measure the entire jet in the emission measurement with a water

jet nozzle diameter of 0.1 mm. The number of photons measured for UTPC is clearly larger than that for MFC.

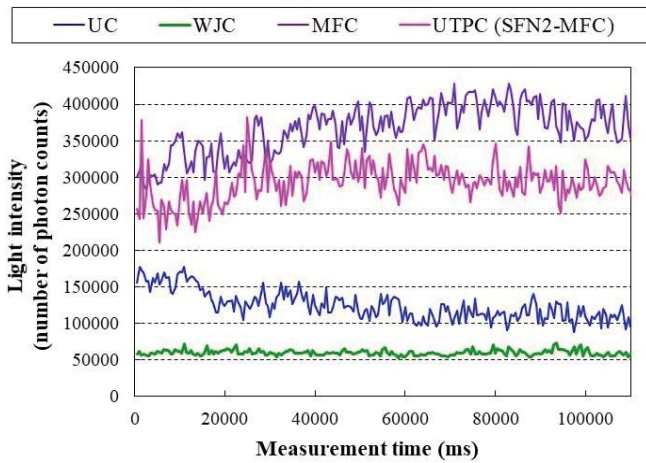


Figure 6. Measurement results of light intensity for various types of cavitation obtained using photon counting head H9319-02.

The relationship between the SFN and light intensity obtained using photon counting head H9319-02 is shown in Figure 7. Similar to the results obtained using photon counting head H9319-01 (Figure 5), SFN2-MFC (two inflow holes) had a higher emission intensity than that of SFN1-MFC (one inflow hole). This is due to the fact that with two holes, the flow velocity in the SFN is higher [22,23] and the size of the WJC bubble, expansion/compression ratio, and temperature in the bubble are increased, which leads to an increase in light intensity.

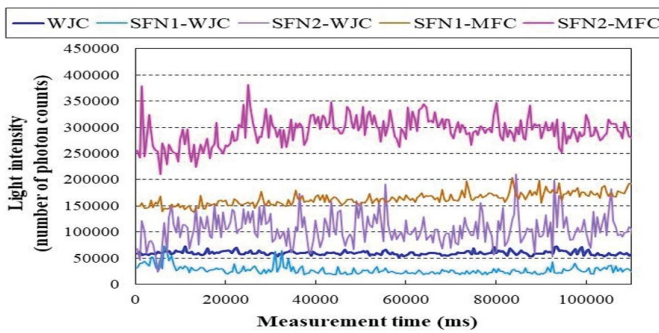


Figure 7. Relationship between SFN and light intensity obtained using photon counting head H9319-02.

The spectrum of SBSL [2] is close to Planck's black-body radiation spectrum [30]. A black body completely absorbs all incident light, and the light emitted from it is determined only by the temperature. Planck introduced the discrete photon energy $h\nu$ to the energy equation of black-body radiation, obtaining the following equation

$$I^{pl} = \frac{2hc^2}{\lambda^5} \frac{1}{\exp\left(\frac{hc}{\lambda k_B T}\right) - 1} \quad (1)$$

where I^{pl} is the energy density ($J \cdot s^{-1} \cdot m^{-2} \cdot sr^{-1} \cdot m^{-1}$), h is Planck's constant ($6.626 \times 10^{-34} Js$), c is the speed of light in the medium (material or vacuum) (m/s), λ is the wavelength (m), k_B is Boltzmann's constant ($1.38 \times 10^{-23} J/K$), and T is the temperature (K). With $c = \lambda \nu$, it can be seen that radiated energy emitted at shorter wavelengths increases more rapidly with temperature than does energy emitted at longer wavelengths. This law may also be expressed in other terms, such as the number of photons emitted at a certain wavelength or the energy density in a volume of radiation. In SBSL, the maximum value in the spectrum shifts toward the ultraviolet region as temperature increases. Figure 8 shows the relationship between the wavelengths of the two detectors and the measurement sensitivity. Photon counting heads H9319-01 and H9319-02 are sensitive

in the wavelength ranges of 270 nm to 640 nm and 270 nm to 840 nm, respectively. It is known that the spectrum of sonoluminescence from cavitation bubbles is very similar to the black-body emission spectrum derived by Planck, in which the maximum value shifts to the low-wavelength ultraviolet region as temperature increases [31]. Therefore, it is considered that photon counting head H9319-01 is more suitable than photon counting head H9319-02 for the photon measurement of hot bubbles.

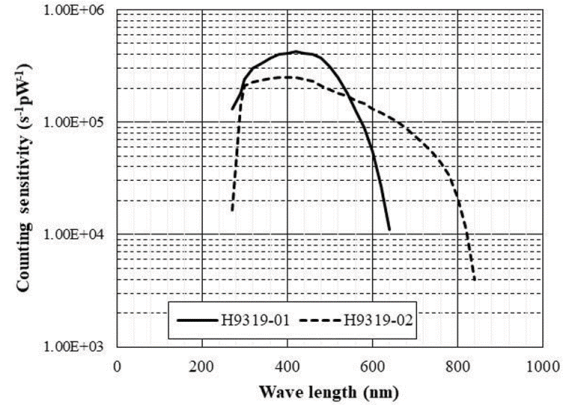


Figure 8. Relationship between wavelength and counting sensitivity for two photon counting heads.

The energy density in Planck's black-body radiation method was corrected using the detector sensitivity of H9319-01 (Figure 9). Due to adiabatic heating in water, the temperature inside the bubble can rise to 2,300-5,100 K for MBSL [32] and 5,000-50,000 K for SBSL [2,33]. Assuming that a UC bubble is 4,000 K, the temperature for each type of cavitation was estimated from the measured light intensity ratio (Figure 9). UTPC (SFN2-MFC) had the highest temperature (4600 K), followed by MFC (4400 K), SFN2-WJC (3750 K), and WJC (3700 K). In previous research, [24] UTPC processing melted ferrite in the pearlite structure in steel (SCM435), whereas low-temperature WJC processing broke the layered structure of pearlite ferrite-cementite. These results are consistent with the present results. In addition, cracks exist just below the surface with WJC, whereas the surface becomes hot with UTPC, so there is a tough layer with no cracks just below the surface of SCM435 steel. This behavior is consistent with the formation of a ductile fracture surface [23]. The temperatures estimated above are temperatures inside the bubble, not on the material surface. Many high-temperature and high-pressure bubbles collide continuously on the material surface and transfer heat to the surface. Regarding the heat transferred by the bubbles to the material surface, some amount is dissipated in the water and some via conduction inside the material. The steady surface temperature is determined by the balance between the heat input to the sample surface and heat radiation. Therefore, for UTPC or MFC processing performed under a given set of conditions, the surface temperature depends on the thermal conductivity of the material and water temperature.

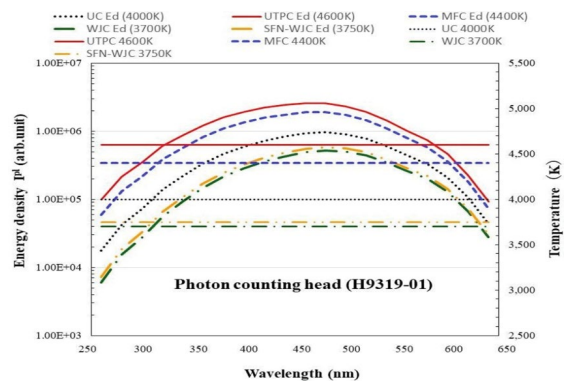


Figure 9. Energy density after detector sensitivity correction and temperature of bubbles for various types of cavitation estimated from measured photon count assuming that UC is 4,000 K (H9319-01).

Table 1 shows the chemical composition of the SCM420 steel used in the present study, which contains chromium and molybdenum. This type of steel is usually classified as heat-resistant steel.

Table 1. Chemical composition of Cr-Mo steel (SCM420).

(Mass%)	C	Si	Mn	P	S	Cu	Ni	Cr	Mo	Fe
SCM420H	0.21	0.25	0.85	0.019	0.016	0.01	0.02	1.1	0.16	Bal.

Figure 10 shows surface photographs of SCM420 steel processed using the various types of cavitation. The light intensity, estimated bubble temperature, and residual stress of SCM420 steel processed using the various types of cavitation are summarized in Table 2. Before cavitation processing, the specimens were mirror polished and blue ink was applied to denote the peening area. Even though UC has a high bubble temperature, it has a low impact pressure and thus almost no ink was removed. For the other cavitation processes, the surface was mostly exfoliated. Some non-exfoliated areas remained in the center of the erosion jet region for SFN-WJC. The mechanical properties of a ring-shaped region slightly away from the central erosion jet region were investigated. The compressive residual stress was in the order SFN2-MFC>WJC>SFN2-WJC>MFC>UC. UC had a higher luminous intensity and corresponding temperature than those for WJC, but had poor high-temperature processing ability due to its small bubble size and small collapse pressure. Cavitation with high luminous intensity (i.e., high temperature) and high pressure during bubble shrinkage had good high-temperature processing ability, improving mechanical strength (e.g., compressive residual stress and hardness) and corrosion resistance (corrosion potential).

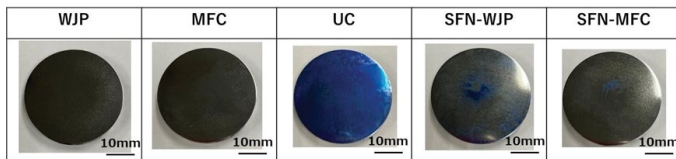


Figure 10. Surface photographs of SCM420 steel processed using various types of cavitation (processing time: 5 min).

Figure 11 shows the Vickers hardness of specimens processed using various types of cavitation. As shown in Table 2, UC results in the smallest hardness. Here, each sample was measured at 10 points, the maximum value and the minimum value were removed, and the average value and standard deviation were obtained. Large variations were found for SFN-WJC. As shown in (Figure 12), WJC resulted in the highest surface roughness. Based on the results of photon measurement, WJC has a low microjet temperature, and is thus a form of cold working. In contrast, UTPC (microforging) has a high-temperature microjet, and is thus a form of hot working. It is considered that the aforementioned observations are due to the unevenness on the surface being leveled and the roughness being reduced by the high-temperature microjet. In addition, UTPC has a higher

temperature than that for MFC, as determined from photon measurement, in addition to having less variation in roughness and thus a uniformly processed material surface.

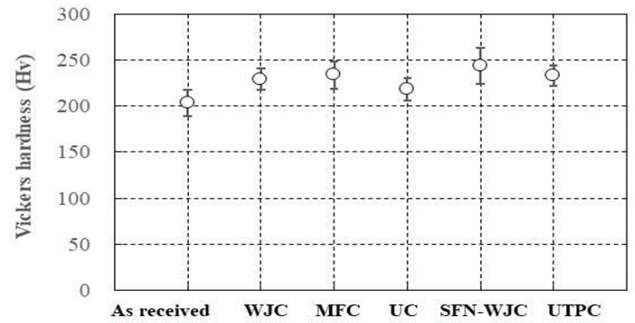


Figure 11. Vickers hardness of specimens processed using various types of cavitation (error bars show standard deviation).

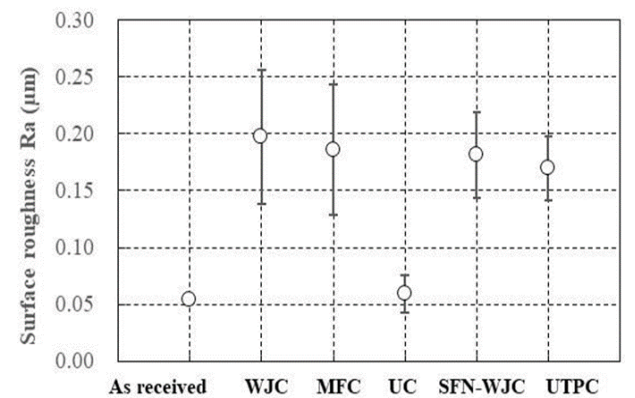


Figure 12. Surface roughness of specimens processed using various types of cavitation (error bars show standard deviation).

The surface potential of specimens processed using the various types of cavitation is shown in Figure 13. Here, the surface potential was measured using Kelvin probe Force Microscopy (KFM). It should be noted that UTPC resulted in the highest surface potential. This is the result of electrochemical action on the surface induced by the high-temperature microjet. The temperature of UTPC is higher than that of MFC, as determined from photon counting. This result is consistent with the data from our previous study, [34] wherein UTPC resulted in a higher surface potential on various materials compared to that obtained with MFC. The reason for this is that the surface potential obtained using KFM corresponds to corrosion resistance. These experimental results therefore suggest that UTPC has a high temperature, is a form of hot working due to the high-temperature and-pressure microjet, and enhances the mechanical and electrochemical properties. Moreover, UTPC had the lowest deviation of surface potential, which indicates uniform hot working on the surface, which is consistent with the results of surface roughness in Figure 12.

Table 2. Light intensity, estimated bubble temperature, and residual stress of SCM420 steel processed using various types of cavitation (processing time: 5 min).

	WJC	MFC	UC	SFN2-WJC	SFN2-MFC (UTPC)
Light intensity (H9319-01)	72,506	2,84,929	1,46,185	85,087	4,07,060
Estimated temperature (K) (H9319-01)	3,700	4,400	4,000	3,750	4,600
Light intensity (H9319-02)	59,653	3,61,468	1,26,024	1,02,140	2,88,474
Estimated temperature (K) (H9319-02)	3,600	4,700	4,000	3,900	4,600
Residual stress (MPa)	-332	-311	-264	-321	-359
Residual stress of as-received (mirror polished) specimen: -242 MPa					

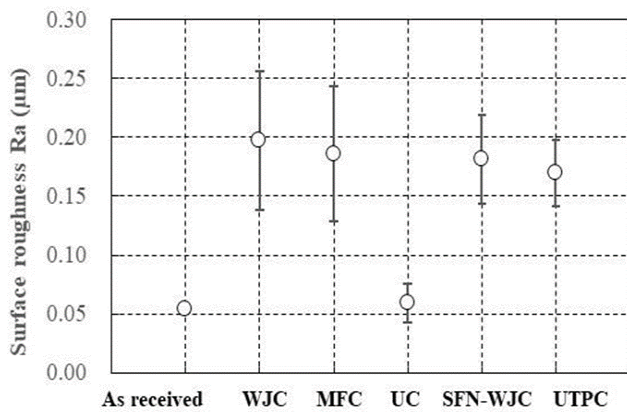


Figure 13. Surface potential of specimens processed using various types of cavitation (error bars show standard deviation).

Conclusion

Sonoluminescence from various types of cavitation bubbles, namely those of WJC, SFN-WJC, MFC, UC, and UTPC, was measured. Sonoluminescence measurements were compared with the surface modification characteristics imparted to Cr-Mo steel. The following results were obtained.

- The luminescence intensity determined using two types of photon counting head, whose detection sensitivity depends on the wavelength range, was in the order WJC<SFN-WJC<UC<MFC<UTPC
- Using Planck's black-body emission method and the light emission intensity (corrected for the sensitivity of the detector), it was possible to estimate the temperature inside the bubbles for various types of cavitation
- The compressive residual stress after cavitation processing was in the order UTPC>WJC>SFN-WJC>MFC>UC. The hardness followed the same order, with UC resulting in the lowest hardness
- UTPC processing, which had the highest emission intensity and temperature, results in small surface roughness with small variation after processing
- The magnitude of luminescence intensity, which was the highest for UTPC, corresponds to the magnitude of corrosion potential (surface potential), which indicates corrosion resistance

Acknowledgment

This research was supported in part by JSPS KAKENHI Grant Number 16K06029 (Grant-in-Aid for Scientific Research (C)) and by the Light Metal Educational Foundation, Inc.

References

1. Minnaert, Marcel. "XVI. On Musical Air-bubbles and the Sounds of Running Water." *London Edinburgh Philos Mag J Sci London, Edinburgh Dublin Philos Mag J Sci* 16 (1933): 235-248.
2. Brenner, Michael P, Sascha Hilgenfeldt, and Detlef Lohse. "Single-Bubble Sonoluminescence." *RMP* 74 (2002): 425.
3. Gompf, B, R Günther, G Nick, and R Pecha, et al. "Resolving Sonoluminescence Pulse width with Time-Correlated Single Photon Counting." *Phys Rev Lett* 79 (1997): 1405.
4. Matula, Thomas J, Ronald A Roy, Pierre D Mourad, and William B. McNamara III, et al. "Comparison of Multibubble and Single-Bubble Sonoluminescence Spectra." *Phys Rev Lett* 75 (1995): 2602.
5. Sehgal, C, RP Steer, RG Sutherland, and RE Verrall. "Sonoluminescence of Argon Saturated Alkali Metal Salt Solutions as a Probe of Acoustic Cavitation." *J Chem Phys* 70 (1979): 2242-2248.

6. Didenko, Yu T, and SP Pugach. "Spectra of Water Sonoluminescence." *J Phys Chem C* 98 (1994): 9742-9749.
7. Giri, Asis, and Vijay H Arakeri. "Measured Pulse Width of Sonoluminescence Flashes in the Form of Resonance Radiation." *Phys Rev E* 58 (1998): R2713.
8. Hiller, Robert A, Seth J Putterman, and Keith R Weninger. "Time-Resolved Spectra of Sonoluminescence." *Phys Rev E* 80 (1998): 1090.
9. DA, Summers, LJ Tyler, J Blaine, and RD Fossey, "Proc. of the Fourth U.S. Water Jet Conference." *The University of California* (1987): 82.
10. Torres, MAS, and HJC Voorwald. "An Evaluation of Shot Peening, Residual Stress and Stress Relaxation on the Fatigue Life of AISI 4340 Steel." *Int J Fatigue* 24 (2002): 877-886.
11. Kikuchi, Shoichi, Yasuhiro Nakahara, and Jun Komotori. "Fatigue Properties of Gas Nitrided Austenitic Stainless Steel Pre-Treated with Fine Particle Peening." *Int J Fatigue* 32 (2010): 403-410.
12. Yoshimura, Toshihiko, K Waseda, K Sato and N Takarayama. "Improvement of Corrosion Resistance of Steel using Mechanochemical Cavitation." *J Fluid Eng-T Asme* 24 (2007): 11.
13. Yoshimura, Toshihiko, and K Sato. "Optimum Injection Pressure of a Cavitating Jet for Introducing Compressive Residual Stress into Stainless Steel." *J Fluid Eng* 31 (2014): 10.
14. Ijiri, Masataka, Daichi Shimonishi, Daisuke Nakagawa, and Toshihiko Yoshimura. "New Water Jet Cavitation Technology to Increase Number and Size of Cavitation Bubbles and its Effect on Pure Al Surface." *Int J Lightweight Mfr* 1 (2018): 12-20.
15. N Saitou, K Enomoto, K Kurosawa, and R Morinaka, et al. "Optimum Injection Pressure of a Cavitating Jet for Introducing Compressive Residual Stress into Stainless Steel." *J Fluid Eng* 20 (2003): 4.
16. Yasui, Kyuichi. "Fundamentals of Acoustic Cavitation and Sonochemistry." In *Theoretical and Experimental Sonochemistry Involving Inorganic Systems.* Springer (2010): 1-29.
17. Yoshimura, Toshihiko, K Tanaka and N Yoshinaga. "Surface Modification of Al by a New Technology Using High Speed Jet in Water Under Ultrasonic Irradiation." *J Fluid Eng* 32 (2016): 10.
18. Yoshimura, Toshihiko, Kumiko Tanaka, and Naoto Yoshinaga. "Proc. of 23rd International Conference Water Jetting, Seattle." *Proc* (2016): 223.
19. Yoshimura, Toshihiko, Kumiko Tanaka, and Naoto Yoshinaga. "Nano-Level Material Processing by Multifunction Cavitation." *Nanoscience and Nanotechnology-Asia* 8 (2018): 41-54.
20. Inventor: Yoshimura, Toshihiko. "Assignee: Sanyo-Onoda City Public University, Patent No.: US 10,590,966 B2, Date of Patent: Mar.17,2020, Method For Generating Mechanical And Electrochemical Cavitation, Method For Changing Geometric Shape And Electrochemical Properties of Substance Surface, Method for Peeling off Rare Metal, Mechanical and Electrochemical Cavitation Generator, and Method for Generating Nuclear Fusion Reaction of Deuterium," Pct Pub. No.: W02016/136656, PCT No.: PCT/JP2016/055016
21. Kling, Charles Lee. "A High Speed Photographic Study of Cavitation Bubble Collapse." *University Michigan* (1970): Report No. 03371-2-T, 08466-7-T.
22. Yoshimura, Toshihiko, Kumiko Tanaka, and Masataka Ijiri. "Nanolevel Surface Processing of Fine Particles by Waterjet Cavitation and Multifunction Cavitation to Improve the Photocatalytic Properties of Titanium Oxide." *Intech Open Cavitation* 10 (2018): 530.
23. Yoshimura, Toshihiko, M Ijiri, D Shimonishi, and K Tanaka. "Micro-Forging and Peening Aging Produced by Ultra-High-Temperature and Pressure Cavitation." *Int J Adv Technol* 9 (2018): 227.
24. Ijiri, Masataka, Daichi Shimonishi, Daisuke Nakagawa, and Toshihiko Yoshimura. "New Water Jet Cavitation Technology to Increase Number and Size of Cavitation Bubbles and its Effect on Pure Al Surface." *Int J Lightweight Mfr* 1 (2018): 12-20.
25. Rayleigh, Lord. "VIII. On the Pressure Developed in a Liquid During the Collapse of a Spherical Cavity." *London Edinburgh Philos Mag J Sci London, Edinburgh Dublin Philos Mag J Sci* 34 (1917): 94-98.
26. Plesset, Milton S. "The Dynamics of Cavitation Bubbles." *J Appl Mech* 16 (1949): 277-282.

27. Ijiri, Masataka, Norihiro Okada, Syouta Kanetou, and Masato Yamamoto, et al. "Thermal Stress Relaxation and High-Temperature Corrosion of Cr-Mo Steel Processed Using Multifunction Cavitation." *Materials* 11 (2018): 2291.
28. Gaitan, D Felipe, Lawrence A Crum, Charles C Church, and Ronald A Roy "Sonoluminescence and Bubble Dynamics for a Single, Stable, Cavitation Bubble." *J Acoust Soc Am* 91 (1992): 3166-3183.
29. Brenner, Michael P, Detlef Lohse, and Todd F Dupont. "Bubble Shape Oscillations and the Onset of Sonoluminescence." *Phys Rev Lett* 75 (1995): 954.
30. Planck, Max. "The Theory of Heat radiation." *Entropie* 144 (1900): 164.
31. Bedaque, Paulo F, Eric Braaten, and H-W. Hammer. "Three-Body Recombination in Bose Gases with Large Scattering Length." *Phys Rev Lett* 85 (2000): 908.
32. Didenko, Yuri T, William B McNamara III, and Kenneth S Suslick. "Molecular Emission from Single-Bubble Sonoluminescence." *Nature* 407 (2000): 877-879.
33. Barber, Bradley P, Robert A Hiller, Ritva Löfstedt, and Seth J Putterman, et al. "Defining the Unknowns of Sonoluminescence." *Phys Rep* 281 (1997): 65-143.
34. Ijiri, Masataka, Daichi Shimonishi, Daisuke Nakagawa, and Toshihiko Yoshimura. "Effect of Water Jet Peening Using Ultrasonic Waves on Pure Al and Al-Cu Alloy Surfaces." *Int J Lightweight Mfr* 1 (2018): 246-251.

How to cite this article: Yoshimura Toshihiko, Daisaku Maeda, Takayuki Ogi, Fumihiko Kato and Masataka Ijiri. "Sonoluminescence from Ultra-High-Temperature and High-Pressure Cavitation and its Effect on Surface Modification of Cr-Mo Steel". *Global J Technol Optim* 11 (2020):240. doi: 10.4172/gjto.2020.11.240